

## Original Article

# In vitro and in vivo study of GSK2830371 and RG7388 combination in liver adenocarcinoma

Chiao-En Wu<sup>1,2,3</sup>, Chiao-Ping Chen<sup>1,2</sup>, Yi-Ru Pan<sup>2,4</sup>, Shih-Ming Jung<sup>5</sup>, John Wen-Cheng Chang<sup>1</sup>, Jen-Shi Chen<sup>1</sup>, Chun-Nan Yeh<sup>2,3,4</sup>, John Lunec<sup>6</sup>

<sup>1</sup>Division of Haematology-Oncology, Department of Internal Medicine, Chang Gung Memorial Hospital, Linkou Branch, Chang Gung University College of Medicine, Taoyuan, Taiwan; <sup>2</sup>Liver Research Center, Chang Gung Memorial Hospital, Linkou, Taoyuan, Taiwan; <sup>3</sup>Institute of Stem Cell and Translational Cancer Research, Chang Gung Memorial Hospital, Linkou, Taoyuan, Taiwan; <sup>4</sup>Department of General Surgery, Chang Gung Memorial Hospital, Linkou Branch, Chang Gung University, Taoyuan, Taiwan; <sup>5</sup>Department of Pathology, Chang-Gung Memorial Hospital, Chang-Gung Children Hospital, Linkou Branch, Chang-Gung University College of Medicine, Taoyuan, Taiwan; <sup>6</sup>Newcastle University Cancer Centre, Bioscience Institute, Medical Faculty, Newcastle University, Newcastle upon Tyne, United Kingdom

Received July 17, 2022; Accepted September 5, 2022; Epub September 15, 2022; Published September 30, 2022

**Abstract:** Intrahepatic cholangiocarcinoma (iCCA) is an adenocarcinoma arising from the intrahepatic bile duct and accounts for the second highest incidence of primary liver cancers after hepatocellular carcinoma. The lack of effective treatment leads to a poor prognosis for advanced iCCA, so new targeted therapy is needed. The impairment of wild-type (WT) p53 tumor suppressor function by its negative regulators frequently occurs in iCCA. Therefore, restoration of WT p53 function by inhibiting its negative regulators is a therapeutic strategy being explored for cancer treatment. Combining an MDM2 inhibitor (MDM2i, RG7388) to stabilize p53 and a WIP1 inhibitor (WIP1i, GSK2830371) to increase p53 phosphorylation enhances p53 function. The combination of MDM2 and WIP1 inhibitors has been reported in several cancer types but *in vivo* studies are lacking. In the current study, liver adenocarcinoma cell lines, RBE and SK-Hep-1, were treated with RG7388 alone and in combination with GSK2830371. Cell proliferation, clonogenicity, protein and mRNA expressions, and cell cycle distribution were performed to investigate the effect and mechanism of growth suppression. To evaluate the antitumor efficacy of RG7388 and GSK2830371 *in vivo*, SK-Hep-1 xenografts in NOD-SCID mice were treated with combination therapy for two weeks. The combination of MDM2i and WIP1i significantly increased the growth inhibition, cytotoxicity, p53 protein expression, and phosphorylation (Ser15), leading to transactivation of downstream targets (p21<sup>WAF1</sup> and MDM2). The *in vivo* results demonstrated that the combination treatment can significantly inhibit tumor growth. In this study, the liver adenocarcinoma cell lines responded to combination treatment via reactivation of p53 function evidenced by increased p53 expression, phosphorylation and expression of its downstream targets. This efficacy was also demonstrated *in vivo*. The current research provides a novel strategy for targeting the p53 pathway in liver adenocarcinoma that warrants further investigation.

**Keywords:** RG7388, GSK2830371, MDM2, WIP1, p53, cholangiocarcinoma

### Introduction

Primary liver cancers include predominantly hepatocellular carcinoma and remaining intrahepatic cholangiocarcinoma (iCCA) [1]. In contrast to extrahepatic cholangiocarcinoma (eCCA), iCCA is an adenocarcinoma arising from bile duct of liver which is a relatively rare but aggressive biliary tract cancer [2]. Prevalence of iCCA is much higher in Asian than in Western

countries [3] possibly because hepatitis virus B, C and flukes are the main etiologies of iCCA in Asian populations [4-6]. iCCA has aggressive biological behavior with high recurrence rate after primary surgery [7-10] and is typically diagnosed at an advanced stage with poor prognosis [11, 12].

Gemcitabine-based chemotherapy is still the standard treatment for iCCA [13, 14]. Previous

clinical trials have evaluated molecular-targeted therapies in combination with chemotherapy but most of them showed disappointing results in large-scale phase III studies [15-17]. Recently, the TOPAZ-1 trial demonstrated that durvalumab in combination with chemotherapy improved overall survival in patients with biliary tract cancer [18]; however, the benefit was marginal (12.8 vs. 11.5 months, hazard ratio [HR] 0.80; 95% confidence interval [CI], 0.66-0.97; P=0.021). Therefore, there is an unmet medical need to explore additional therapeutic agents or strategies for iCCA.

The tumor suppressor protein p53, encoded by the *TP53* gene, is responsible for DNA repair, cell cycle arrest, apoptosis and cell senescence leading to cancer suppression and death [19, 20]. However, cancers frequently have impaired wild-type (WT) p53 function due to either *TP53* mutation or dysregulation of its negative regulators which enhance cancer cell development, survival, and proliferation [21]. The principal negative regulators of WTp53 are mouse double minute 2 homolog (MDM2) and wild-type p53-induced phosphatase 1 (WIP1). Targeting MDM2 and WIP1 with small molecule inhibitors (MDM2i and WIP1i) to activate the p53 pathway is a novel therapeutic strategy in cancer treatment, particularly in p53<sup>WT</sup> cancers [22-24]. The activity of RG7388 (idasanutlin) as MDM2i was explored across various indications was explored across various indications [25, 26]. GSK2830371, a WIP1i, was designed for inhibition of WIP1 protein leading to increased p53 phosphorylation [27]. We have previously reported anti-cancer activity of MDM2i in combination with GSK2830371 in cutaneous melanoma [22] and liver adenocarcinoma [23] by increasing the function and stability of p53 in a p53-dependent manner. This strategy has been studied in a range of cancers [28-30], however, no *in vivo* studies have been reported for this combination. Therefore, we have investigated the *in vitro* and *in vivo* pre-clinical activity of RG7388 and GSK2830371 in iCCA to explore the potential for future clinical trials.

## Materials and methods

### Cell lines and compounds

RBE [31] and SK-Hep-1 [32] were purchased from the RIKEN Cell Bank (Ibaraki, Japan) and

authenticated by the STR (short tandem repeat) method. These cell lines were cultured in RPMI medium 1640 (Gibco) and DMEM (Gibco) containing 10% FBS respectively. RG-7388 MDM2i was obtained from Roche under a material transfer agreement (MTA). GSK-2830371 WIP1i was purchased from Sigma-Aldrich. All compounds were dissolved in DMSO and used at a final concentration of 0.5% DMSO with minimal cytotoxic effects on cells.

### Growth inhibition assay

Cells were seeded as 3000 cells/well in 96-well plates overnight before 72-hour and 96-hour treatment with RG7388 and GSK2830371, both individually and in combination. CCK8 tetrazolium based redox reagent (Dojindo Molecular Technologies, Inc., Kumamoto, Japan) was used according to the manufacturer's instructions and absorbance optical density (OD) was measured at 450 nm wavelength using a microplate reader. The GI<sub>50</sub> value was determined and the detailed calculation of GI<sub>50</sub> was presented in our previous report [23].

### Clonogenic assay

Cell lines were seeded in 6-well plates with different cell densities depending on the cell lines (RBE 800/well and SK-Hep1 200/well) for 96 hours before treatment with RG7388, combined with or without GSK2830371 for 72 hours. Fresh medium was replaced and the cells were fixed when colonies were visible depending on the growth rates of the cells (usually 3-4 days). The IC<sub>50</sub> values for reduction in clonogenic survival were determined [23].

### RNA extraction and qRT-PCR

Cell lines were seeded in 6-well plates and treated with RG7388 and GSK2830371, either alone or in combination for 6 and 24 hours. Cells were harvested and total RNA was extracted using TRI Reagent (Sigma). RNA purity and concentration were estimated with an ND-1000 spectrophotometer (NanoDrop Technologies, Thermo Scientific, UK). Complementary DNA (cDNA) was generated using the HiScript I<sup>TM</sup> First Strand cDNA Synthesis Kit (Bionovas) as described by the manufacturer. qRT-PCR was carried out using SYBR green RT-PCR master mix (Life Technologies) as per the manufacturer's guidelines and the following primers:

## RG7388 and GSK2830371 in cholangiocarcinoma

MDM2: F-AGTAGCAGTGAATCTACAGGGA, R-CTGATCCAACCAATCACCTGAAT; CDKN1A: F-TGTCCGTCAGAACCCATGC, R-AAAGTCGAAGTTCCATCGCTC; GAPDH: F-GTCTCCTCTGACTTCAACAGC, R-ACCACCTGTTGCTGTAGCCAA. qRT-PCR reactions using a total of 25 ng of the cDNA samples per 20  $\mu$ L final reaction volume, transcriptional levels were determined by QS5 system using SYBR green system (Applied Biosystems, Thermo Scientific). GAPDH was used as endogenous control and samples of cells exposed to DMSO solvent control were used as the calibrator for each independent repeat experiment. Analysis was carried out using QuantStudio™ Design & Analysis Software.

### Immunoblotting

After cells were seeded in 6-well plates and treated with RG7388 alone and in combination with GSK2830371 for 6 and 24 hours, cell lysates were harvested by Pierce™ RIPA Lysis and Extraction buffer (Thermo Scientific) with Protease and Phosphatase Inhibitor (Roche) on ice and stored at temperature of -20°C. Protein concentration was measured by a Pierce™ bicinchoninic acid kit (Thermo Scientific). Equal quantities of protein were then separated by SDS-polyacrylamide gel electrophoresis. The separated proteins were then orthogonally transferred by electrophoresis and immobilized onto Amersham™ nitrocellulose membranes (GE Healthcare Life Science). Primary antibodies against p53 (DO-7) (#GTX34938, GeneTex), phospho-p53 (Ser-15) (#9284, Cell Signaling Technology), MDM2 (2A10) (#MABE281, Merck Millipore), p21<sup>WAF1</sup> (12D1) (#2947, Cell Signaling Technology), WIP1 (F-10) (#sc-376257, Santa Cruz Biotechnology), GAPDH (GT239) (#GTX627408, GeneTex) and secondary goat anti-mouse or anti-rabbit horseradish peroxidase-conjugated antibodies (#115-035-003/#111-035-003, Jackson ImmunoResearch Laboratories) were used, as appropriate for the corresponding primary. All antibodies were diluted in 5% (w/v) non-fat milk in TBS-Tween. Proteins were visualized using enhanced chemiluminescence (Merck Millipore) and image capture system (UVP ChemStudio PLUS).

### Fluorescence-activated cell sorting (FACS)

Cells were seeded in 6-well plates and treated with RG7388 alone and in combination with GSK2830371 for 24 and 48 hours. Both float-

ing and adherent cells were collected and fixed using 70% cold ethanol. Samples were incubated in propidium iodide (PI)/RNase Staining Solution (Cell Signaling) for 20 minutes in the dark at room temperature, then were analyzed on a FCSCalibur™ flow cytometer using CellQuest Pro software (Becton Dickinson, Oxford, UK). Cell cycle distribution based on DNA content was determined using FlowJo vX software.

### Xenograft tumorigenicity

To evaluate the efficacy of combination treatment *in vivo*, SK-Hep-1 cells were used to produce xenografts in mice. In brief,  $5 \times 10^6$  tumor cells in 50  $\mu$ L PBS were injected into 4-week-old NOD/SCID mice subcutaneously. When the tumors grew to average 100 mm<sup>3</sup>, RG7388 (80 mg/kg, two times per day on days 1-5 and 8-12 during the treatment period), GSK2830371 (75 mg/kg, two times per day [27]) and combinations were applied for two weeks. Tumor size, tumor volume, and body weight of mouse were measured during the 2-week treatment and then for 4 weeks after treatment. Tumors were harvested after completion of study (6 weeks).

### Statistical analysis

Data were presented as mean  $\pm$  standard error of mean (SEM) unless otherwise stated. Statistical tests were carried out using GraphPad Prism 6 software and *p*-values represent unpaired t-tests or two-way ANOVA analysis. A *p*-value less than 0.05 was considered as statistically significant.

## Results

### GSK2830371 potentiated the growth inhibitory activity of RG7388

Minimal growth inhibitory activity of 10  $\mu$ M GSK2830371 was found in RBE and SK-Hep-1 cells in our previous study [23]. A combination index to examine the synergism between two compounds can only be performed when both agents have a dose-dependent effect [33], therefore, potentiation rather than synergy was examined in the following experiments. A fixed concentration of 2.5  $\mu$ M GSK2830371 was selected to evaluate the potentiation of RG7388 by GSK2830371 when used in combination. SK-Hep-1 and RBE were treated with RG7388 alone or in combination with 2.5  $\mu$ M

## RG7388 and GSK2830371 in cholangiocarcinoma

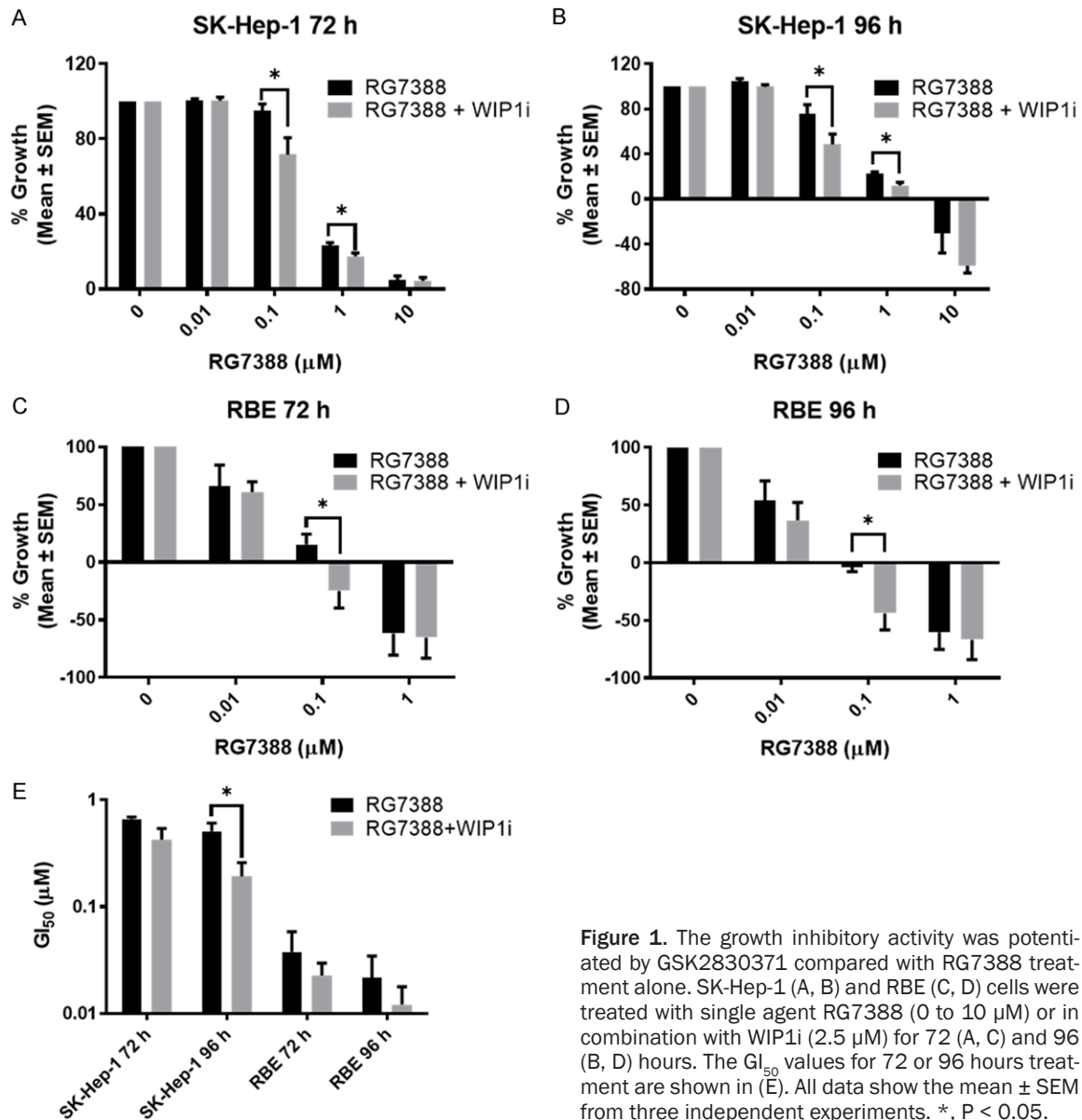


**Figure 1.** The growth inhibitory activity was potentiated by GSK2830371 compared with RG7388 treatment alone. SK-Hep-1 (A, B) and RBE (C, D) cells were treated with single agent RG7388 (0 to 10  $\mu\text{M}$ ) or in combination with WIP1i (2.5  $\mu\text{M}$ ) for 72 (A, C) and 96 (B, D) hours. The GI<sub>50</sub> values for 72 or 96 hours treatment are shown in (E). All data show the mean  $\pm$  SEM from three independent experiments. \*,  $P < 0.05$ .

GSK2830371 for 72 and 96 hours and cell proliferation was measured by CCK-8 assay (Figure 1A-D). The % growth inhibition of combination treatment was normalized to any effect of GSK2830371 alone. GSK2830371 significantly increased growth inhibitory activity of RG7388, which was evidenced by increased growth inhibition and cytotoxic activity. Numerically lower GI<sub>50</sub> values for combination treatment compared with RG7388 monotherapy was also noted (Figure 1E). Furthermore, we also tested the growth inhibitory effect of RG7388 monotherapy in a panel of BTC cell lines, and most of them had no growth inhibi-

tory activity except SK-Hep-1 and RBE (Figure S1). The small effect of RG7388 at the highest dose (10  $\mu\text{M}$ ) was potentially an off-target effect.

### *GSK2830371 potentiated the cytotoxic activity of RG7388*

If the OD value in the proliferation assay after treatment was less than the OD at day 0, subtraction of the day 0 OD value produced negative value, which indicated the compound or combination was not only cytostatic but also cytotoxic. Figure 1A-D demonstrated that combination therapy not only resulted in greater

## RG7388 and GSK2830371 in cholangiocarcinoma

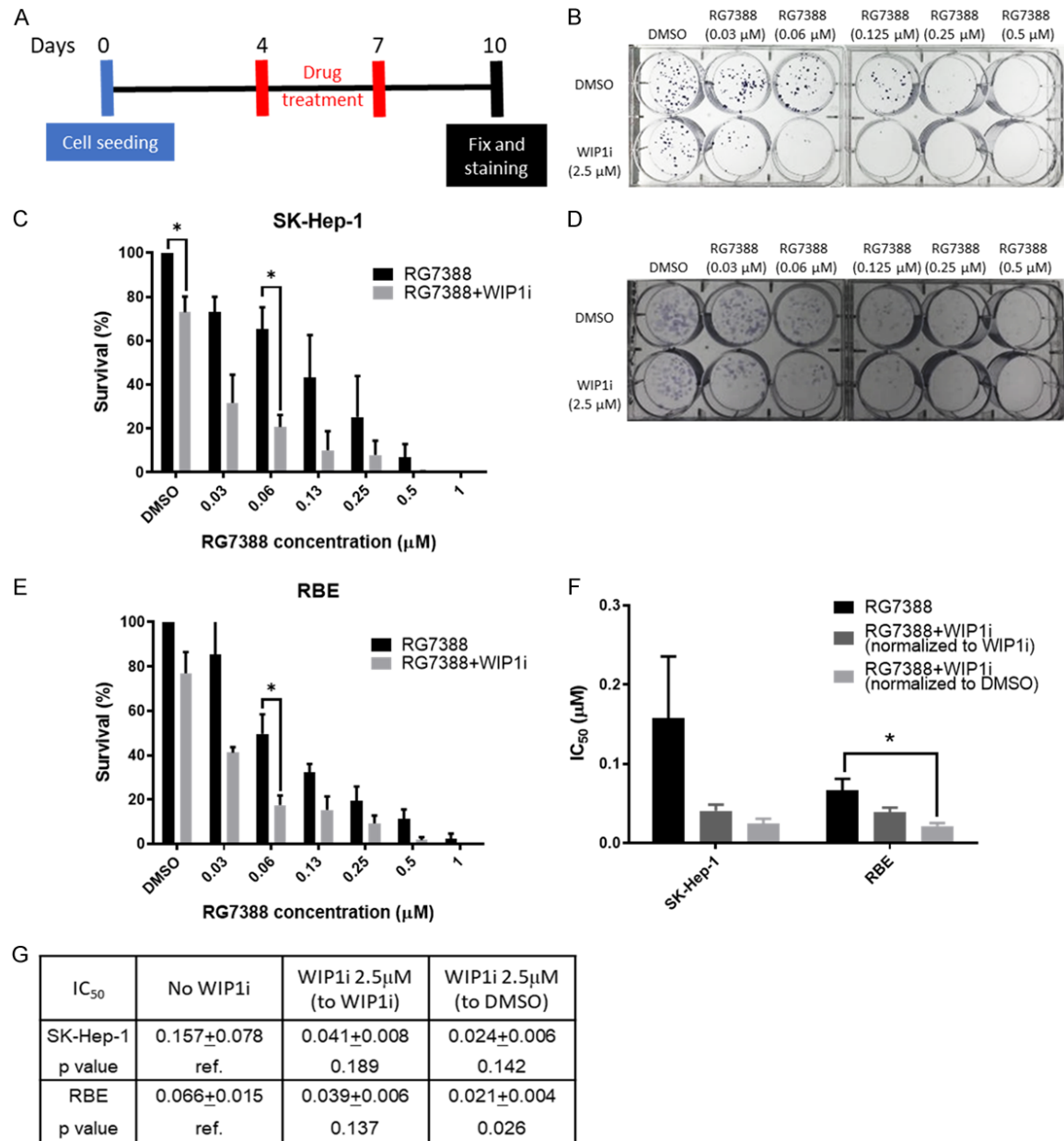


**Figure 2.** GSK2830371 combination with RG7388 enhanced the inhibition of colony formation compared with RG7388 monotherapy. (A) Schema for experiment timeline. Colony formation was strongly repressed after MD-M2i and WIP1i treatment in SK-Hep-1 (B, C) and RBE (D, E) cells. The IC<sub>50</sub> values are summarized in (F) and a detailed table of results normalized to DMSO or WIP1i is shown in (G). \*, P < 0.05. All data exhibited the mean ± SEM from three independent experiments.

inhibition of proliferation but also greater cytotoxic activity than RG7388 monotherapy. In addition, a clonogenic assay was performed to evaluate whether GSK2830371 potentiation of the cytotoxic activity of RG7388 was also reflected in reduced colony formation (Figure 2). As shown in Figure 2, fewer colonies were formed after combination treatment compared

with RG7388 treatment alone, indicating that the addition of GSK2830371 significantly reduced the clonogenic survival of RBE and SK-Hep-1 cells compared with the effect of RG7388 alone (Figure 2B-E). The IC<sub>50</sub> values of RG7388 for colony number reduction were calculated after normalization to either GSK-2830371 or DMSO and shown in Figure 2F, 2G.

## RG7388 and GSK2830371 in cholangiocarcinoma

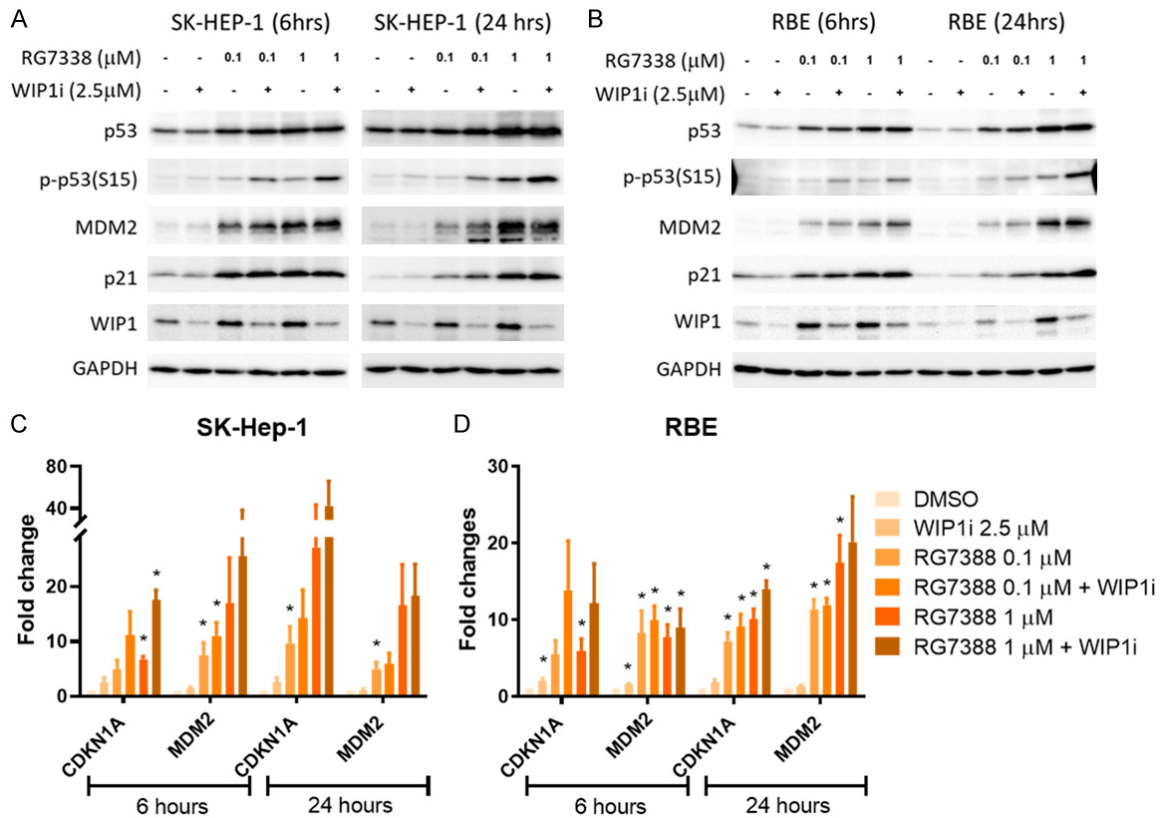


**Figure 3.** Phosphorylation of p53 (Ser15) and protein expression of p53 target genes induced by MDM2i and WIP1i monotreatment or when combined. Protein expression of p53, p-p53 (Ser15), p21, MDM2, and WIP1 after RG7388 (0.1 or 1 μM) and/or GSK2830371 treatment at 6 and 24 hours was detected by Western blot in SK-Hep-1 (A) and RBE (B). Cells treated with the same conditions were collected and their mRNA expression for *CDKN1A* and *MDM2* were determined by RT-qPCR (C, D). \*, P < 0.05. All data show the mean ± SEM for three independent experiments.

These results indicated GSK2830371 not only potentiated the growth inhibition but also the reduction in clonogenic cell survival induced by RG7388.

### GSK2830371 induced p53 phosphorylation and stabilization via WIP1 inhibition

To confirm the on-target effects of the combination of RG7388 and GSK2830371 and explore the possible mechanism, RBE and SK-Hep-1 were treated with RG7388, GSK2830371, or a combination of both compounds for 6 and 24 hours. Immunoblotting showed RG7388 stabilized p53, leading to increased p53 detection after 6-hour treatment and the increased p53 persisted for 24 hours (Figure 3A, 3B). MDM2, p21 and WIP1 are all transcriptional targets of p53 and expression of these proteins increased at 6 hour and the increases persisted for 24 hours. When GSK2830371 was added to RG7388 treatment, decreased WIP1 protein

and correspondingly increased phosphorylated p53 (Ser15) was observed, indicating the on-target effect of GSK2830371. Compared to RG7388 monotreatment, no significant changes in total p53 protein after combination treatment were evident, but increases in p53 targets, p21 and MDM2, were found (Figure 3A, 3B). Similar findings were noted for both RBE and SK-Hep-1 treated with two doses of RG7388 (0.1 μM and 1 μM) with or without GSK2830371 (2.5 μM) for 6 and 24 hours. Moreover, the p53 transcriptional target gene protein products were evident at the earlier time point of four hours after 0.1 μM RG7388 in combination with GSK2830371 treatment (Figure S2).

Dose-dependent increases in p53 target gene transcripts were also found using qRT-PCR (Figure 3C, 3D). Furthermore, combination treatment induced significantly more mRNA transcripts of *CDKN1A* (encoding p21) and

## RG7388 and GSK2830371 in cholangiocarcinoma

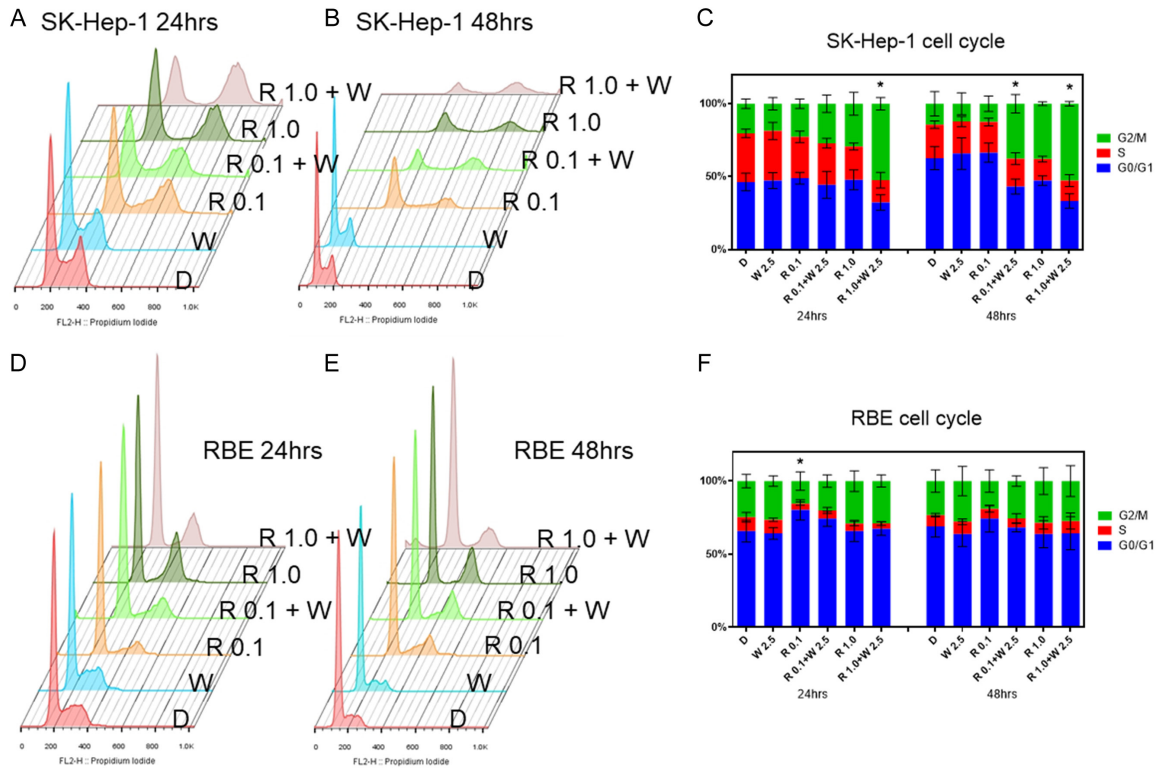


**Figure 4.** G2 phase arrest was induced by RG7388 treatment in combination with GSK2830371. The cell cycle distribution was assayed by FACS. The histogram profiles show the cell cycle distribution detected by staining with PI (A, B, D, and E). The cell cycle distributions from at least 3 independent replicates were summarized in (C) (SK-Hep-1) and (F) (RBE). D, DMSO; W, WIP1i; R, RG7388. \*,  $P < 0.05$  by two-way ANOVA compared to control group. All data show the mean  $\pm$  SEM from three independent experiments.

*MDM2* than RG7388 monotherapy. The fold increases of p53 target gene transcripts were cell-line and time dependent. For SK-Hep-1, *MDM2* increased more than *CDKN1A* after 6-hour treatment but *CDKN1A* induction was higher than *MDM2* after 24-hour treatment. In contrast, RBE expressed higher levels of *CDKN1A* mRNA after 6-hour treatment and higher levels of *MDM2* mRNA after 24-hour treatment.

### *GSK2830371 induced more G2 arrest in combination with RG7388*

RBE and SK-Hep-1 cells were treated with two doses of RG7388 (0.1  $\mu$ M and 1  $\mu$ M) and GSK2830371 (2.5  $\mu$ M) for 24 and 48 hours and FACS were performed to evaluate the cell cycle distribution after RG7388 with or without GSK2830371 treatment. Comparing to DMSO treatment, GSK2830371 (2.5  $\mu$ M) demonstrated minimal effects on cell cycle distribution in RBE and SK-Hep-1. For SK-Hep-1 cells, 0.1  $\mu$ M

RG7388 induced both G1 and G2 arrest and decreased S phase, and 1  $\mu$ M RG7388 induced more G2 arrest. GSK2830371 markedly increased the G2 arrest when it was added to RG7388 (Figure 4A-C). A similar pattern was found with RBE cells. For RBE 0.1  $\mu$ M RG7388 induced only G1 arrest and 1  $\mu$ M RG7388 induced G2 arrest. GSK2830371 again induced further G2 arrest when it was added to 0.1  $\mu$ M RG7388 but not 1  $\mu$ M RG7388 (Figure 4D-F).

### *In vivo xenograft evaluation of RG7388 and GSK2830371 combination*

The schedule of treatment and sacrifice of mice was summarized in Figure 5A. RG7388 (80 mg/kg, day 1-5 and 8-12) and/or GSK2830371 (75 mg/kg, day 1 to 14) [27] were administered by oral gavage for two weeks. The tumor weight on sacrifice from the mice after 2-weeks treatment and 4-weeks subsequent follow-up are shown in Figure 5B and summarized in Figure 5C. Both RG7388 and GSK2830371

## RG7388 and GSK2830371 in cholangiocarcinoma

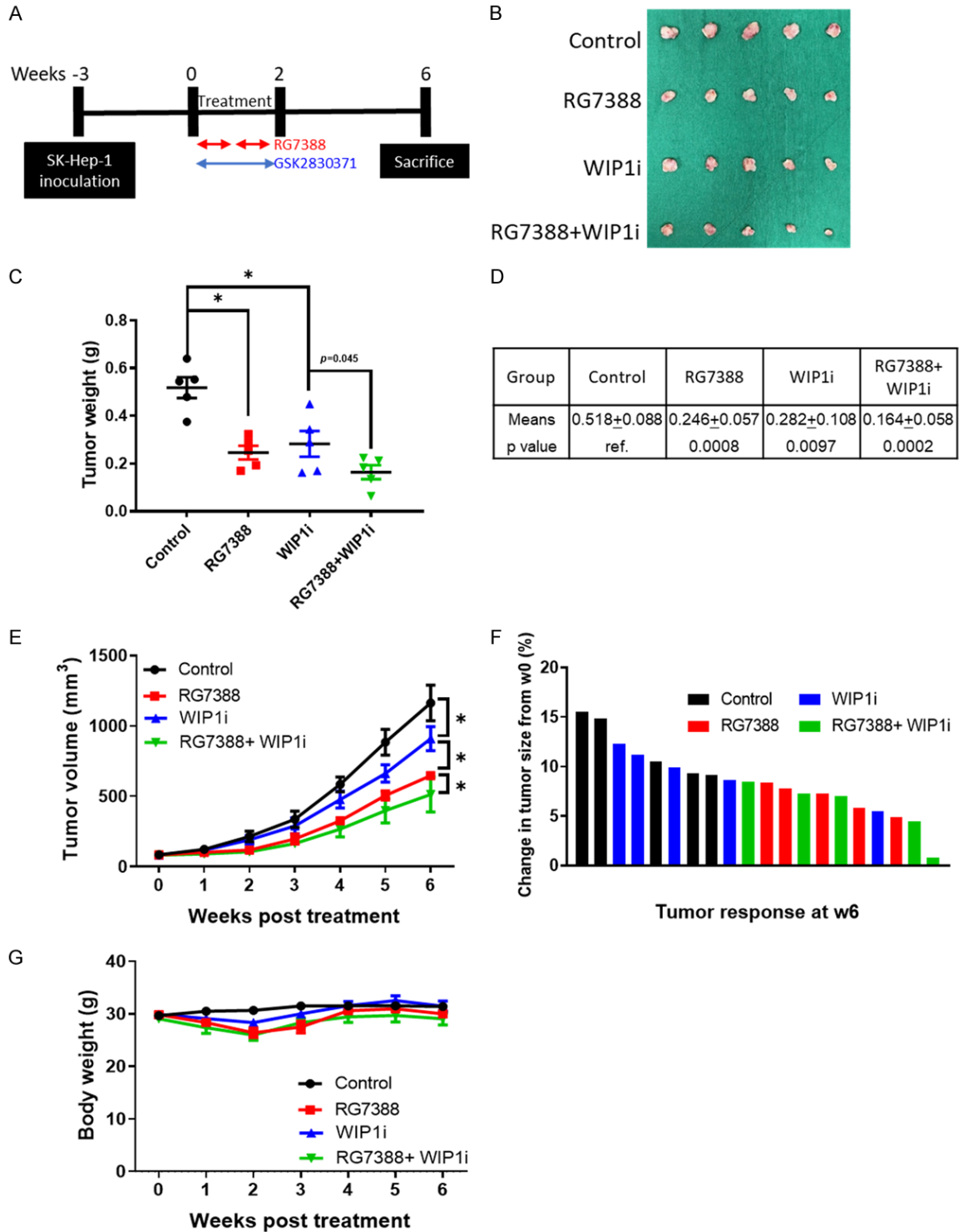


**Figure 5.** WIP1i and MDM2i combination restricted tumor growth *in vivo*. (A) Schema for experiment timeline. Mice were treated with RG7388 on days 1-5 and days 8-12, and GSK2830371 on days 1-14 during the treatment period for two weeks. (B, C) Tumor size and weight showed maximum reduction with the combination treatment. (D) A detailed table of results with the means, standard errors, and *p* values was displayed from (C). (E) Tumor growth was significantly suppressed to a greater extent with GSK2830371 combined with RG7388 than with either inhibitor alone. The *p* value was calculated by two-way ANOVA. (F) Waterfall plot of tumor response for each tumor (n=5/group) at week 6 compared with week 0. There was minimal alteration in body weight in all groups; except the RG7388 and/or WIP1i group at week two, which subsequently recovered (G). Scale bar =100  $\mu$ m. \*, *P* < 0.05 by unpaired t-test in (C). All data exhibited the mean  $\pm$  SEM (n=5).

significantly reduced the tumor sizes comparing to control. The combination of RG7388 and GSK2830371 significantly decreased the tumor sizes compared with GSK2830371 monotreatment. The combination treatment resulted in some smaller retrieved tumors than RG7388 monotreatment, even though the average difference did not achieve statistical significance at the 95% confidence level (**Figure 5C**). Significant reductions in tumor weight were observed for the mice treated with RG7388 or GSK2830371. RG7388 ( $n=5$ ,  $P=0.0008$ ) significantly reduced the tumor growth rates compared to GSK2830371 ( $n=5$ ,  $P=0.0097$ ), which was compatible with *in vitro* findings. Furthermore, the combination of RG7388 and GSK2830371 significantly inhibited the tumor growth more than RG7388 monotherapy ( $n=5$ ,  $P=0.0398$ ) (**Figure 5D**). Tumor growth curves were also evaluated from tumor size measurements by calipers every week after the initiation of treatment (**Figure 5E**). Maximum tumor growth in control and GSK2830371 groups at the endpoint compared with week zero as shown in **Figure 5F**. The body weight was slightly reduced during the treatment period except for the control group, but they soon returned to normal during the post-treatment follow-up time (**Figure 5G**).

## Discussion

Targeting negative regulators of p53 may provide a novel therapeutic strategy in the treatment of advanced BTC [24]. Previously, we reported *in vitro* studies demonstrating the potential of such a strategy using HDM201 and GSK2830371 treatment of BTC cell lines [23]. RG7388, an MDM2 inhibitor which stabilizes p53 leading to cell cycle arrest and growth inhibition, has been studied in a number of clinical trials. In the current study, we demonstrated that GSK2830371 targeting the WIP1 phosphatase oncoprotein enhanced RG7388 activity via increased p53 phosphorylation and resulted in profound growth inhibition. Importantly, this is the first *in vivo* study to investigate the combination of MDM2i and WIP1i in cancer.

Both RBE and SK-Hep-1 cell lines we have used are p53 wild-type. It is well established that MDM2 inhibitors are ineffective against mutant p53 cells, and we and others have previously

shown that the potentiation of MDM2 inhibitors by inhibition of WIP1 is also p53-dependent [22, 23]. Also, clinical trials of MDM2 inhibitors use wild-type p53 tumor status as a patient selection criterion [24, 34], hence we have chosen these cell lines which are wild-type for p53. Although the basal levels of MDM2 in both cell lines were low (**Figure 3A, 3B**), targeting p53 by MDM2i is still effective treatment. Except for MDM2-amplified cell lines, the basal levels of MDM2 and p53 are usually low in p53 wild-type cell lines as both MDM2 and p53 are tightly regulated and turning over at a high rate [35, 36]. Elevated p53 activates MDM2 leading to autoregulatory feedback p53 degradation. However, when MDM2i blocks this interaction p53 continues to be produced but is released from degradation without the negative control by MDM2, consequently p53 levels rise and then continue to transcribe MDM2 resulting in elevated MDM2 protein levels. However, the increased MDM2 continues to be prevented by the inhibitor to bind to p53 and the increasing feedback loop becomes futile. The net result is an increase in both the p53 and MDM2 protein levels. Although p53 can regulate many genes based on previous reports [22, 23], we only investigated the major representative genes p21 and MDM2. Based on previous reports, the induction of some p53-regulated genes is cell line dependent, however, CDKN1A and MDM2 are consistently detected major transcriptional targets of p53 intimately involved in its growth inhibitory and autoregulatory function. CDKN1A is the most investigated p53 target gene and has been causally shown to be responsible for p53-induced cell cycle arrest.

GSK2830371 has been reported to enhance p53-mediated tumor suppression by MDM2 inhibitors, nutlin-3 [29, 37], nutlin-3a [38], HDM201 [23] and RG7388 [29] or by chemotherapy [27, 37]. GSK2830371 has been shown to potentiate MDM2 inhibitors via increased p53 phosphorylation, acetylation, and decreased ubiquitination, resulting in increased growth inhibition and cytotoxic activity for melanoma cells [22]. Although p53 phosphorylation (Ser15), the substrate of WIP1, is not essential for p53 activity, it can lead to increased stabilization of p53 as a result of decreased ubiquitination [22]. GSK2830371 has also been shown to potentiate the effect of RG7388 on liver adenocarcinoma cells [23]. In extension of previ-

ous studies, we explored and validated the combination of RG7388 and GSK2830371 in liver cholangiocarcinoma cells using *in vitro* assays and *in vivo* models.

Although activation of p53 leads to cell cycle arrest and apoptosis, the fate of cells from p53 reactivation may be cancer- or cell-dependent [22, 39]. The underlying mechanisms that determine cell fate following p53 activation and the choice between cell cycle arrest, senescence or apoptosis are incompletely understood. In the current study, no apoptotic responses were found by either FACS analysis or caspase 3/7 activity with either RBE or SK-Hep-1 cells after RG7388 treatment, either with or without combination treatment with GSK2830371 (data not shown) which was consistent with previous findings for liver cancer cell lines [39].

In conclusion, the current study demonstrated that combination treatment with MDM2 and WIP1 inhibitors, RG7388 and GSK2830371, may have some benefit for CCA. This study reports the first *in vivo* results of this novel combination in a xenograft system. As more than half of BTC are WT p53 [24], these promising results warrant further investigation aimed towards supporting the case for future clinical trials.

### Acknowledgements

This work was supported by grants from Linkou Chang-Gung Memorial Hospital (NMRP-G3K6201, NZRPG3K0221, CMRPG3K0601, CMRPG3J0971~2 and CRRPG3K0021, CMRPG3L0911~3, CMRPG3M0521 to CEW, CMRPG3I0241~3, CORPG3J0251~2, CRRPG3K0011, CRRPG3K0031 and CMRPG3K0711 to CNY) and the Ministry of Science and Technology (109-2314-B-182-080-MY3 and 110-2811-B-182-525 to CEW).

### Disclosure of conflict of interest

None.

**Address correspondence to:** Chun-Nan Yeh, Department of General Surgery, Chang Gung Memorial Hospital at Linkou, Chang Gung University College of Medicine, 5, Fu-Hsing Street, Kwei-Shan, Taoyuan, Taiwan. Tel: +886-3-3281200; Fax: +886-2871-2121 Ext. 2508; E-mail: yehchunna@gmail.com;

John Lunec, Newcastle University Cancer Centre, Bioscience Institute, Medical Faculty, Newcastle University, Newcastle upon Tyne, United Kingdom. Tel: +044-0191-208-4420; Fax: +044-0191-208-4301; E-mail: john.lunec@newcastle.ac.uk

### References

- [1] Bosch FX, Ribes J, Díaz M and Cléries R. Primary liver cancer: worldwide incidence and trends. *Gastroenterology* 2004; 127: S5-S16.
- [2] Razumilava N and Gores GJ. Cholangiocarcinoma. *Lancet* 2014; 383: 2168-2179.
- [3] Blechacz B. Cholangiocarcinoma: current knowledge and new developments. *Gut Liver* 2017; 11: 13-26.
- [4] Maroni L, Pierantonelli I, Banales JM, Benedetti A and Marzioni M. The significance of genetics for cholangiocarcinoma development. *Ann Transl Med* 2013; 1: 28.
- [5] Ong CK, Subimerb C, Pairojkul C, Wongkham S, Cutcutache I, Yu W, McPherson JR, Allen GE, Ng CC, Wong BH, Myint SS, Rajasegaran V, Heng HL, Gan A, Zang ZJ, Wu Y, Wu J, Lee MH, Huang D, Ong P, Chan-on W, Cao Y, Qian CN, Lim KH, Ooi A, Dykema K, Furge K, Kukongviriyapan V, Sripa B, Wongkham C, Yongvanit P, Futreal PA, Bhudhisawasdi V, Rozen S, Tan P and Teh BT. Exome sequencing of liver fluke-associated cholangiocarcinoma. *Nat Genet* 2012; 44: 690-693.
- [6] Seo JW, Kwan BS, Cheon YK, Lee TY, Shim CS, Kwon SY, Choe WH, Yoo BC, Yoon JM and Lee JH. Prognostic impact of hepatitis B or C on intrahepatic cholangiocarcinoma. *Korean J Intern Med* 2020; 35: 566-573.
- [7] Nakachi K, Konishi M, Ikeda M, Mizusawa J, Eba J, Okusaka T, Ishii H, Fukuda H and Furuse J. A randomized phase III trial of adjuvant S-1 therapy vs. observation alone in resected biliary tract cancer: Japan Clinical Oncology Group Study (JCOG1202, ASCOT). *Jpn J Clin Oncol* 2018; 48: 392-395.
- [8] Chan KM, Tsai CY, Yeh CN, Yeh TS, Lee WC, Jan YY and Chen MF. Characterization of intrahepatic cholangiocarcinoma after curative resection: outcome, prognostic factor, and recurrence. *BMC Gastroenterol* 2018; 18: 180.
- [9] Jan YY, Yeh CN, Yeh TS, Hwang TL and Chen MF. Clinicopathological factors predicting long-term overall survival after hepatectomy for peripheral cholangiocarcinoma. *World J Surg* 2005; 29: 894-898.
- [10] Yeh CN, Wang SY, Chen YY, Chen MH, Chiang KC, Cheng CT, Tsai CY, Wang CC, Yeh TS and Chen TC. A prognostic nomogram for overall survival of patients after hepatectomy for intrahepatic cholangiocarcinoma. *Anticancer Res* 2016; 36: 4249-4258.

## RG7388 and GSK2830371 in cholangiocarcinoma

- [11] Shaib Y and El-Serag HB. The epidemiology of cholangiocarcinoma. *Semin Liver Dis* 2004; 24: 115-125.
- [12] Hung TH, Hung JT, Wu CE, Huang Y, Lee CW, Yeh CT, Chung YH, Lo FY, Lai LC, Tung JK, Yu J, Yeh CN and Yu AL. Globo H is a promising therapeutic marker for intrahepatic cholangiocarcinoma. *Hepatol Commun* 2022; 6: 194-208.
- [13] Valle J, Wasan H, Palmer DH, Cunningham D, Anthoney A, Maraveyas A, Madhusudan S, Iveson T, Hughes S, Pereira SP, Roughton M and Bridgewater J. Cisplatin plus gemcitabine versus gemcitabine for biliary tract cancer. *N Engl J Med* 2010; 362: 1273-1281.
- [14] Wu CE, Chou WC, Hsieh CH, Chang JW, Lin CY, Yeh CN and Chen JS. Prognostic and predictive factors for Taiwanese patients with advanced biliary tract cancer undergoing frontline chemotherapy with gemcitabine and cisplatin: a real-world experience. *BMC Cancer* 2020; 20: 422-422.
- [15] Hezel AF, Deshpande V and Zhu AX. Genetics of biliary tract cancers and emerging targeted therapies. *J Clin Oncol* 2010; 28: 3531-3540.
- [16] Zhu AX and Hezel AF. Development of molecularly targeted therapies in biliary tract cancers: reassessing the challenges and opportunities. *Hepatology* 2011; 53: 695-704.
- [17] Sahu S and Sun W. Targeted therapy in biliary tract cancers-current limitations and potentials in the future. *J Gastrointest Oncol* 2017; 8: 324-336.
- [18] Oh DY, He AR, Qin S, Chen LT, Okusaka T, Vogel A, Kim JW, Suksombooncharoen T, Lee MA, Kitano M, Burris Iii HA, Bouattour M, Tanasanvimon S, Zaucha R, Avallone A, Cundom J, Rokutanda N, Xiong J, Cohen G and Valle JW. A phase 3 randomized, double-blind, placebo-controlled study of durvalumab in combination with gemcitabine plus cisplatin (GemCis) in patients (pts) with advanced biliary tract cancer (BTC): TOPAZ-1. *J Clin Oncol* 2022; 40: 378-378.
- [19] Wade M, Wang YV and Wahl GM. The p53 orchestra: Mdm2 and Mdmx set the tone. *Trends Cell Biol* 2010; 20: 299-309.
- [20] Levine AJ, Momand J and Finlay CA. The p53 tumour suppressor gene. *Nature* 1991; 351: 453-456.
- [21] Muller PA and Vousden KH. p53 mutations in cancer. *Nat Cell Biol* 2013; 15: 2-8.
- [22] Wu CE, Esfandiari A, Ho YH, Wang N, Mahdi AK, Aptullahoglu E, Lovat P and Lunec J. Targeting negative regulation of p53 by MDM2 and WIP1 as a therapeutic strategy in cutaneous melanoma. *Br J Cancer* 2018; 118: 495-508.
- [23] Wu CE, Huang CY, Chen CP, Pan YR, Chang JW, Chen JS, Yeh CN and Lunec J. WIP1 inhibition by GSK2830371 potentiates HDM201 through enhanced p53 phosphorylation and activation in liver adenocarcinoma cells. *Cancers (Basel)* 2021; 13: 3876.
- [24] Wu CE, Pan YR, Yeh CN and Lunec J. Targeting P53 as a future strategy to overcome gemcitabine resistance in biliary tract cancers. *Biomolecules* 2020; 10: 1474.
- [25] Mascarenhas J, Passamonti F, Burbury K, El-Galaly TC, Gerds A, Gupta V, Higgins B, Wonde K, Jamois C, Kovic B, Huw LY, Katakam S, Maffioli M, Mesa R, Palmer J, Bellini M, Ross DM, Vannucchi AM and Yacoub A. The MDM2 antagonist idasanutlin in patients with polycythemia vera: results from a single-arm phase 2 study. *Blood Adv* 2022; 6: 1162-1174.
- [26] Corbali MO and Eskazan AE. Idasanutlin as a new treatment option in improving the therapeutic odyssey of relapsed/refractory AML. *Future Oncol* 2020; 16: 887-889.
- [27] Gilmartin AG, Faitg TH, Richter M, Groy A, Seefeld MA, Darcy MG, Peng X, Federowicz K, Yang J, Zhang SY, Minthorn E, Jaworski JP, Schaber M, Martens S, McNulty DE, Sinnamon RH, Zhang H, Kirkpatrick RB, Nevins N, Cui G, Pietrak B, Diaz E, Jones A, Brandt M, Schwartz B, Heerding DA and Kumar R. Allosteric Wip1 phosphatase inhibition through flap-subdomain interaction. *Nat Chem Biol* 2014; 10: 181-187.
- [28] Chen Z, Wang L, Yao D, Yang T, Cao WM, Dou J, Pang JC, Guan S, Zhang H, Yu Y, Zhao Y, Wang Y, Xu X, Shi Y, Patel R, Zhang H, Vasudevan SA, Liu S, Yang J and Nuchtern JG. Wip1 inhibitor GSK2830371 inhibits neuroblastoma growth by inducing Chk2/p53-mediated apoptosis. *Sci Rep* 2016; 6: 38011.
- [29] Esfandiari A, Hawthorne TA, Nakjang S and Lunec J. Chemical inhibition of wild-type p53-induced phosphatase 1 (WIP1/PPM1D) by GSK2830371 potentiates the sensitivity to MDM2 inhibitors in a p53-dependent manner. *Mol Cancer Ther* 2016; 15: 379-391.
- [30] Chamberlain V, Drew Y and Lunec J. Tipping growth inhibition into apoptosis by combining treatment with MDM2 and WIP1 inhibitors in p53(WT) uterine leiomyosarcoma. *Cancers (Basel)* 2021; 14: 14.
- [31] Enjoji M, Sakai H, Nawata H, Kajiyama K and Tsuneyoshi M. Sarcomatous and adenocarcinoma cell lines from the same nodule of cholangiocarcinoma. *In Vitro Cell Dev Biol Anim* 1997; 33: 681-683.
- [32] Heffelfinger SC, Hawkins HH, Barrish J, Taylor L and Darlington GJ. SK HEP-1: a human cell line of endothelial origin. *In Vitro Cell Dev Biol* 1992; 28A: 136-142.
- [33] Chou TC. Drug combination studies and their synergy quantification using the Chou-Talalay method. *Cancer Res* 2010; 70: 440-446.

## RG7388 and GSK2830371 in cholangiocarcinoma

- [34] Montesinos P, Beckermann BM, Catalani O, Esteve J, Gamel K, Konopleva MY, Martinelli G, Monnet A, Papayannidis C, Park A, Récher C, Rodríguez-Veiga R, Röllig C, Vey N, Wei AH, Yoon SS and Fenaux P. MIRROS: a randomized, placebo-controlled, Phase III trial of cytarabine ± idasanutlin in relapsed or refractory acute myeloid leukemia. *Future Oncol* 2020; 16: 807-815.
- [35] Momand J, Zambetti GP, Olson DC, George D. and Levine AJ. The mdm-2 oncogene product forms a complex with the p53 protein and inhibits p53-mediated transactivation. *Cell* 1992; 69: 1237-45.
- [36] Oliner JD, Pietsenpol JA, Thiagalingam S, Gvuris J, Kinzler KW and Vogelstein B. Oncoprotein Mdm2 conceals the activation domain of tumor suppressor-p53. *Nature* 1993; 362: 857-860.
- [37] Pechackova S, Burdova K, Benada J, Kleiblova P, Jenikova G and Macurek L. Inhibition of WIP1 phosphatase sensitizes breast cancer cells to genotoxic stress and to MDM2 antagonist nutlin-3. *Oncotarget* 2016; 7: 14458-14475.
- [38] Sriraman A, Radovanovic M, Wienken M, Najafova Z, Li Y and Dobbelstein M. Cooperation of Nutlin-3a and a Wip1 inhibitor to induce p53 activity. *Oncotarget* 2016; 7: 31623-31638.
- [39] Xue W, Zender L, Miething C, Dickins RA, Hernandez E, Krizhanovsky V, Cordon-Cardo C and Lowe SW. Senescence and tumour clearance is triggered by p53 restoration in murine liver carcinomas. *Nature* 2007; 445: 656-660.

RG7388 and GSK2830371 in cholangiocarcinoma

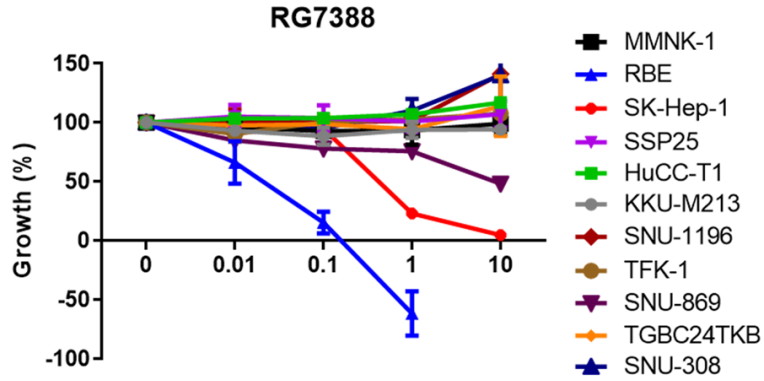


**Figure S1.** The effect of RG7388 (0 to 10  $\mu$ M) treatment on cell proliferation for 72 hours in a panel of BTC cell lines.

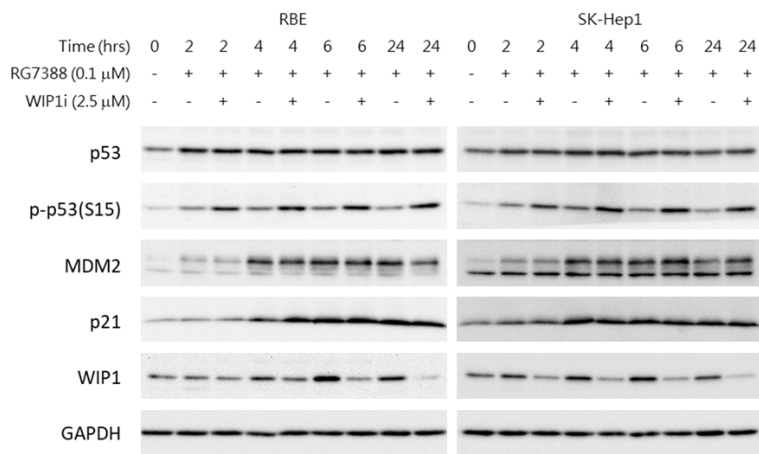


**Figure S2.** Protein expression of p53, p-p53 (Ser15), p21, MDM2, and WIP1 during RG7388 (0.1  $\mu$ M) and/or GSK2830371 (2.5  $\mu$ M) treatment at 0, 2, 4, 6, and 24 hours detected by Western blot in SK-Hep-1 and RBE cells.